RISE controller for class I of underactuated mechanical systems: Design and Real-Time Experiments

Afef Hfaiedh, Ahmed Chemori, Afef Abdelkrim

RISE controller for class I of underactuated mechanical systems: Design and Real-Time Experiments

Afef Hfaiedh[1, a *], Ahmed Chemori [2,b] and Afef Abdelkrim[1,c]

[1]LARA, Automatique, ENICARTHAGE, Ecole Nationale d'Ingénieurs de Carthage, Tunisia.
[2]LIRMM, Université de Montpellier-CNRS, France
[a] *Afefhfaiedh@hotmail.fr,*
[b]*Ahmed.chemori@lirmm.fr,*
[c]*Afef.a.abdelkrim@ieee.org*

ABSTRACT— *In this paper, RISE Controller (Robust Integral of the Sign of the Error) is proposed for class I of Underactuated mechanical systems. This class is characterized by two degrees of freedom and one control input. This approach is based on a global change of coordinates where the system is transformed into cascade strict feedback form. Through this transformation, two novel desired trajectories are proposed for the design of the controller.*

Experimentally, implementation of this approach has some drawbacks. Most of real systems are only equipped with position sensors (i.e. encoders). Velocities and accelerations are usually non-measurable. Indeed, the RISE controller is depending on the first derivative of the position measurement of the system. Furthermore, experimental quantities contain a noisy measurement and the latter is amplified in the computation of the velocity in real time. This may decrease the performance of the closed loop system. To overcome, these drawbacks, a HOSM differentiator is used to estimate, the velocity measurement of the system.

To validate the effectiveness of this approach, extensive real-time experiments are conducted for the stabilization of the Inertia Wheel Inverted Pendulum (IWIP), where the system is under unmatched disturbances.

KEYWORDS: Nonlinear RISE-based control design, HOSM differentiator, Underactuated mechanical system, Inertia Wheel Inverted Pendulum.

1. Introduction

In recent years, control of Underactuated Mechanical Systems (UMS) has got growing attention. For the same configuration, an (UMS) requires less control than fully actuated system. This feature decreases the weight, allows eliminating certain control devices and reduces the cost of conception. Furthermore, the control of such system presents a control solution in case of an actuator failure. It guarantees the good operation of the system and ensures the continuity of difficult missions [1].

Although, (UMS) invokes challenges that are not found in fully actuated systems. It presents a restriction which makes the procedure of the control more complicated. When some degrees of freedom are not directly driven by actuators, a higher nonlinear coupling between actuated and non actuated coordinates makes the control design difficult. This class of system is often called a non-minimum phase system because the zero dynamic is unstable. Among the control difficulties of this class is the lack of feedback linearizability and classical control techniques cannot be directly applied to the system.

UMSs are studied on case by case. There is no general theory or common approach to control all kind of underactuated mechanical systems. Some researchers were focused on the classification of some known examples of underactuated systems. Using the method of control flow diagram, Seto and Baillieul proposed three structures namely chain, tree and isolated vertex [2]. These obtained structures present the interaction forces through the degrees of freedom. Several control approaches were proposed for this type of classification, like backstepping, sliding mode, for more details see [1].

Another classification is based on the structural properties of the system like (interacting inputs, kinetic symmetry, etc) was proposed by [3].

Using explicit change of coordinates for system with two degrees of freedom, three normal forms were identified called feedback form, feed-forward form and non-triangular linear quadratic form. The author proposed a backstepping procedure for the first form and a forwarding scheme for the second form.

More of this classification, a wide range of control approaches have been proposed in the literature, partial feedback linearization [4], passivity [5] [6], adaptive neural network-based controller [7], stable limit cycle generation [8] to name a few.

The sliding mode control (SMC) has received widespread attention in control of underactuated mechanical systems. It is insensitive to external disturbances and has a finite-time transient. After a transformation of the system dynamics into a quasi-chained form, a nonlinear robust controller is developed in [9] [10] to make the system state variables staying in the sliding manifold, and vanishing asymptotically towards the equilibrium point. In [11], a combination of a high-gain observer and a first-order sliding-mode controller was proposed for the stabilization of the inertia wheel inverted pendulum. A change of coordinates was made in order to obtain the normal form. Then the system is decoupled into linear and non-linear subsystems. A high-gain observer is used for the estimation of the states. However, classical sliding mode controllers are characterized by a higher frequency switching known as the "chattering phenomenon", causing dangerous damages to the actuators.

In this paper, we are interested on implementing another robust controller which belongs to the set of sliding mode controllers, namely the Robust Integral Signum of Error (RISE) controller [12]. The proposed approach is related to the class I of underactuated mechanical systems defined in [3]. Many theoretical extensions and practical applications of this control strategy have been reported in literature. And it was applied to a wide variety of systems including autonomous underwater vehicle [13], Multi-Link Flexible Manipulator [14], parallel robot [15], a servo system of a Hard Disc Drive (HDD) [16]. In general case, this control was applied to a fully actuated mechanical system and cannot be applied directly to an underactuated mechanical system. We proceed by several steps. Firstly, we refer to the change of coordinates presented in [3]. This change of coordinates transforms the system on strict feedback form. This transformation simplifies the control design. It decouples the original system in two subsystems, where a new control input appears in the actuated subsystem and don't have effect on the unactuated subsystem. Secondly we define a new desired trajectories and error tracking according to the new transformation. Then, we design the RISE controller using the error tracking and its first derivative. Using this method experientially in an underactuated benchmark, a chattering phenomenon is observed in the control input. Indeed, the position control is a noisy signal, and its derivative is calculated by numerical derivation in real time. This is amplifying the noise in the velocity signal, likewise the control input. To overcome this problem, we decide to estimate the velocity using a second order differentiator. This control schema is validated in real time in a well known underactuated benchmark system namely the inertia wheel inverted pendulum.

In the second section, we present a general background on transformation of system in strict feedback form and introduce the application of RISE controller using such transformation. The section 3, we apply this control schema to stabilize the inertia wheel inverted pendulum. In the next section, we present experimental results and attest the advantages of using a differentiator to estimate states of the system. Conclusion and future work are given in section 5.

2. Class I of underactuated mechanical systems

The general mathematical model of underactuated mechanical systems with two degrees of freedom is described by

$$m_{11}(q)\ddot{q}_1 + m_{12}(q)\ddot{q}_2 + h_1(q,\dot{q}) = \tau_1 \quad (1)$$

$$m_{21}(q)\ddot{q}_1 + m_{22}(q)\ddot{q}_2 + h_2(q,\dot{q}) = \tau_2 \quad (2)$$

There are two modes of actuation defined depending on the application.

- (A_1) $\tau = \tau_2 \in \mathbb{R}$ is the control input and $\tau_1 = 0$.
- (A_2) $\tau = \tau_1 \in \mathbb{R}$ is the control input and $\tau_2 = 0$.

The mode (A_1) represents the class I of underactuated mechanical system. The TORA, the Acrobot and the Inertia Wheel Inverted Pendulum (IWIP) belong to the mode (A_1), whereas the inverted pendulum is actuated under the mode (A_2). Underactuated mechanical systems of class I can be transformed in strict feedback form.

In this paper, we are interested in the mode (A_1). The dynamic of the system can be partially linearized into a double integrator due the lack of control input in the first equation (1). The linearization procedure is called collocated partial feedback linearization. Subsequently, we present the transformation of the system in strict feedback form.

Definition 1: A nonlinear system is in strict feedback form, has the following triangular structure.

$$\dot{z}_1 = f(z, \xi_1) \quad (3)$$
$$\dot{\xi}_1 = \xi_2 \quad (4)$$
$$\dot{\xi}_{n-1} = \xi_n \quad (5)$$
$$\dot{\xi}_n = u \quad (6)$$

2.1. RISE controller: Application to class I of underactuated mechanical systems

In this section, we provide the details to design a RISE controller for class I of underactuated mechanical systems. The first step consists on transforming the system in strict feedback using a global change of coordinates.

2.1.1. Strict feedback linearization

Underactuated mechanical system of class I with two degrees of freedom can be transformed into cascade nonlinear system in strict feedback form.

Assuption1: Using the lagrangian of the system, and if the quantity $m_{11}^{-1}(q_2)m_{12}(q_2)$ is integrable, a global change of coordinates can be obtained.

$$z_1 = q_1 + \gamma(q_2) \quad (7)$$
$$\gamma(q_2) = \int_0^{q_2} m_{11}^{-1}(\theta)m_{12}(\theta)\partial\theta \quad (8)$$
$$z_2 = m_{11}(q_2)p_1 + m_{12}(q_2) \quad (9)$$
$$\xi_1 = q_2 \quad (10)$$
$$\xi_2 = p_2 \quad (11)$$

Then, the following global change of coordinates obtained from the Lagrangian of the system, transforms the dynamic of the system into a cascade nonlinear system in strict feedback form. The obtained cascaded system is an interconnection of a linear (double integrator) subsystem, and a nonlinear core subsystem.

The backstepping procedure has proven to be successful for this type of transformation system [3]. The system is transformed as follow

$$\dot{z}_1 = m_{11}^{-1}(\xi_1)z_2 \quad (12)$$
$$\dot{z}_2 = g_1(z_1 - \gamma(\xi_1), \xi_1) \quad (13)$$
$$\dot{\xi}_1 = \xi_2 \quad (14)$$
$$\dot{\xi}_2 = u \quad (15)$$

where $g_1(q_1, q_2) = -\frac{\partial V(q)}{\partial q_1}$, $V(q)$ is the potential energy of the system and u is the new control from collocated partial feedback linearization. The torque and the new control are related through this relation

$$\tau = \alpha(q)u + \beta(q, \dot{q}) \quad (16)$$
$$\alpha(q) = m_{22}(q) - m_{21}(q)m_{11}^{-1}(q)m_{12}(q) \quad (17)$$
$$\beta(q, \dot{q}) = h_2(q, \dot{q}) - m_{21}(q)m_{11}^{-1}(q)h_1(q, \dot{q}) \quad (18)$$

2.1.2. RISE control design

Our objective, is the control of class I underactuated mechanical system. The following hypotheses are essential to ensure the design of RISE controller.

Consider a nonlinear system with dynamics of the following form

$$m(x)\ddot{x} + f(x) = u \quad (19)$$

where u is the control input vector, m and f are uncertain nonlinear functions.

Assuption2: The uncertain nonlinear system matrix m is bounded from below by a positive constant $\underline{m}$ and from above by a non decreasing positive function $\overline{m}$. The following inequality holds:

$$\underline{m}\|\xi\|^2 \leq \xi^T m\xi \leq \overline{m}\|\xi\|^2 \quad (20)$$

Assuption3: The nonlinear functions m and f are second-order differentiable.

Assuption4: The desired reference trajectory is continuously differentiable with respect to time.

To design the RISE controller, we need auxiliary error signals, denoted by $e_i(t), i = \{1,2\}$ and defined in the following manner.

$$e_1 \triangleq q_d - q \quad (21)$$
$$\dot{e}_1 \triangleq \dot{q}_d - \dot{q} \quad (22)$$
$$e_2 \triangleq \dot{e}_1 + \alpha_1 e_1 \quad (23)$$
$$r \triangleq \dot{e}_2 + \alpha_2 e_2 \quad (24)$$

where α_1 and α_2 are positive constant gains. q_d is the desired trajectory tracking and $\dot{q}_d$ is the derivative of the desired position. $r(t)$ cannot be used in the control design. It requires the measurement of the derivative error $e_2$which depends on the acceleration measurement. The equation of the control input is given by [13] as follow

$$u = (k_s + 1)e_2 - (k_s + 1)e_2(0) + v_f \quad (25)$$
$$\dot{v}_f = (k_s + 1)\dot{e}_2 + \beta sign(e_2) \quad (26)$$
$$v_f(0) = 0 \quad (27)$$

where k_s and β are positive constant gains and the $sign$ is the Signum function.

2.2. Robust Levant differentiator

HOSM differentiators were developed in order to provide the derivatives required to implement HOSM controllers. They are known for their robustness in presence of noise and their exactness in its absence.

$$\dot{w}_0 = v_0 \quad (28)$$
$$v_0 = w_0 - \lambda_2 L^{\frac{1}{3}}|w_0 - y|^{\frac{2}{3}} sign(w_0 - y) \quad (29)$$
$$\dot{w}_1 = v_1 \quad (30)$$
$$v_1 = w_1 - \lambda_1 L^{\frac{1}{2}}|w_1 - v_0|^{\frac{1}{2}} sign(w_1 - v_0) \quad (31)$$
$$\dot{w}_2 = -\lambda_0 L sign(w_2 - v_1) \quad (32)$$

If $t = 0, w_0 = y$ and $w_1(0) = w_2(0) = 0$. y is the output to be estimated, w_0 is its estimated. w_1 and $w_2$are its first and second derivative. λ_0, $\lambda_1$and λ_2 are positive gains. In the next section, we design a control input for the inertia wheel inverted pendulum. We use the HOSM differentiator to estimate states of the system.

3. Application example : IWIP

The proposed RISE control scheme for the Inertia wheel inverted pendulum is presented in this section. The description of the system and design of the proposed control scheme are presented.

3.1. The inertia wheel inverted pendulum

The inertia wheel inverted pendulum is a flat underactuated mechanical system with two degrees of freedom and one control input. The joint $\theta_1$between the frame and the pendulum body is unactuated (passive). The joint between the body and the inertia wheel θ_2 is actuated (active). The unstable equilibrium point corresponds to the position in which the pendulum is pointed upwards. In absence of a control force, the pendulum is unable to maintain this position indefinitely. To ride up the pendulum, the torque generated by the sum of the gravity $P$and the force F^-must be lower than the applied torque acting at O, and generated by the force F^+ see figure 1. The motor torque of the rotating wheel produces an angular acceleration, which generates torque acting on the pendulum. Therefore, the goal is to find control acting on the inertia wheel to bring the pendulum from its initial position to its unstable equilibrium point and to maintain it, in spite of external disturbances.

The dynamical model of IWIP is obtained by using the Euler–Lagrange method. The Lagrangian formulation for this system is given by

$$L = \frac{1}{2}\left(I_1\dot{\theta}_1^2 + i_2(\theta_1 + \theta_2)^2\right) - m_0 g cos(\theta_1) \quad (33)$$

The dynamic model of the IWIP is described by

$$\begin{bmatrix} I+i_2 & i_2 \\ i_2 & i_2 \end{bmatrix} \begin{bmatrix} \ddot{\theta}_1 \\ \ddot{\theta}_2 \end{bmatrix} - \begin{bmatrix} m_0 g sin(\theta_1) \\ 0 \end{bmatrix} = \begin{bmatrix} 0 \\ \tau \end{bmatrix} \quad (34)$$

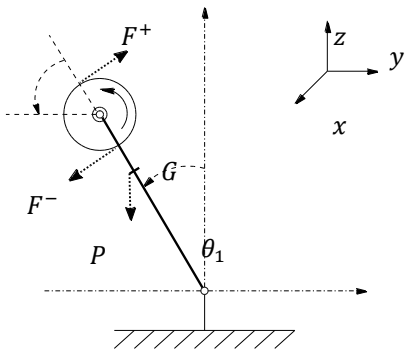

Figure 1. *Schematic view of the inertia wheel inverted pendulum: the first joint θ_1 is unactuated, while the second joint θ_2 is actuated.*

where $\theta = [\theta_1, \theta_2]$, is the vector of generalized positions, τ is the torque applied by the actuator on the inertia wheel. The parameters of the system are summarized in table 1.

$$I = m_1 {l_1}^2 + m_2 {l_2}^2 + i_1 \quad (35)$$
$$m_0 = m_1 l_1 + m_2 l_2 \quad (36)$$

Table 1. *Dynamic parameters of the IWIP*

Parameter	Description	Unit
$\boldsymbol{\theta_1}$	Pendulum angle with respect to vertical axis	rad
$\boldsymbol{\theta_2}$	Wheel angle with respect to pendulum axis	rad
$\boldsymbol{i_1}$	Rotational Inertia of pendulum	$kg.m^2$
$\boldsymbol{i_2}$	Rotational Inertia of Wheel	$kg.m^2$
$\boldsymbol{m_1}$	Mass of the pendulum	kg
$\boldsymbol{m_2}$	Mass of the Wheel	kg
$\boldsymbol{l_1}$	Length from pendulum base to pendulum center of mass	m
$\boldsymbol{l_2}$	Length from pendulum base to Wheel center of mass	m
$\boldsymbol{g}$	Constant of gravitational acceleration	m/s^2

3.2. Control design

In accordance with the theorem (4.2.1) in [3], the global change of coordinates is defined by

$$z_1 = \frac{\partial L}{\partial \dot{\hat{\theta}}_1} = (I + i_2)\dot{\hat{\theta}}_1 + i_2 \dot{\theta}_2 \quad (37)$$

$$z_2 = \hat{\theta}_1 \quad (38)$$
$$z_3 = \theta_2 \quad (39)$$

where $z = [z_1, z_2, z_3]$ is the novel state, $\hat{\theta}_1$ and $\dot{\hat{\theta}}_1$ are the estimated angular position and estimated angular velocity of the pendulum through the HOSM differentiator.

Using the Lagrangian formulation, the system is transformed to a cascade form as follows

$$\dot{z}_1 = \frac{\partial L}{\partial \theta_1} = m_0 g sin(z_2) \quad (40)$$

$$\dot{z}_2 = \frac{z_1}{I+i_2} - \frac{i_2 z_3}{I+i_2} \quad (41)$$

$$\dot{z}_3 = u \quad (42)$$

The angular position of the rotating wheel is not used as a state in the new transformation, for the reason that, it does not play any role in the dynamic and does not appear in the lagrangian equation. z_2 is a virtual control input of the $z_1$subsystem. Using a sigmoidal function $-\arctan(z_1)$ for the $z_1$subsystem can globally asymptotically stabilizes (37), by choosing this valid Lyapunov function $V(z_1) = \frac{z_1^2}{2}$.

So, using the novel transformation, two novel desired trajectories are defined. They are described as follows

$$\theta_{1d} = z_{2d} = -\arctan(z_1) \tag{43}$$

$$\dot{\theta}_{1d} = \frac{m_0 g sin(z_2)}{(1+(z_1^2))} \tag{44}$$

To design the control schema, we need to define the error tracking using the novel desired trajectories and the estimates states.

$$\hat{e}_1 = \hat{\theta}_1 - \theta_{1d} \tag{45}$$
$$\dot{\hat{e}}_1 = \dot{\hat{\theta}}_1 - \dot{\theta}_{1d} \tag{46}$$
$$\hat{e}_2 = \dot{\hat{e}}_1 + \alpha_1 \hat{e}_1 \tag{47}$$

Using the equation (16)-(18), (25) and (26) the control input is described as follow

$$\tau = \frac{i_2 I}{(i_2+I)} u + \frac{i_2 m_0 g\ sin(\hat{\theta}_1)}{(i_2+I)} \tag{48}$$

$$u = (k_s + 1)\hat{e}_2 - (k_s + 1)\hat{e}_2(0) + v_f \tag{49}$$
$$\dot{v}_f = (k_s + 1)\hat{e}_2 + \beta sign(\hat{e}_2) \tag{50}$$

Figure 2 presents the block diagram of the proposed control approach.

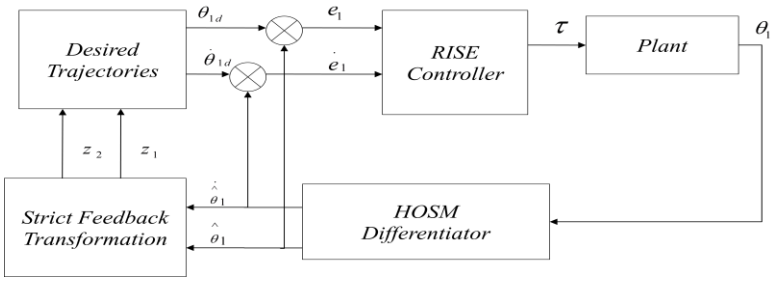

Figure 2. View of the block diagram of the proposed control approach

4. Experimental results

The efficiency of the controller is confirmed by real time experiments, carried out on the testbed of the inertia wheel inverted pendulum (IWIP), designed and developed at LIRMM . Figure 3 presents the experimental testbed of (IWIP).

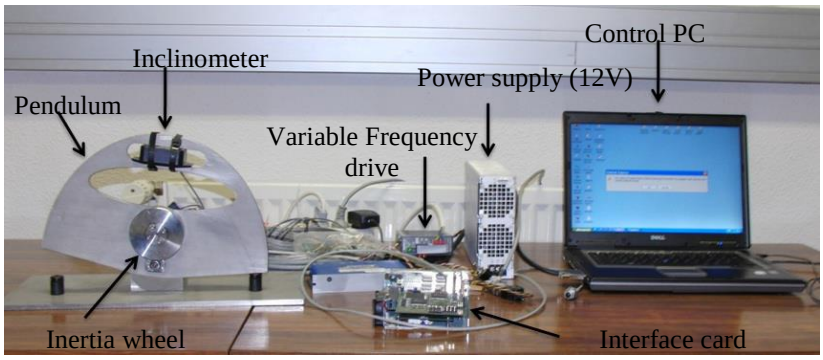

Figure 3. View of the IWIP experimental testbed

Due to mechanical stops, the pendulum angle θ_1, is constrained to remain within the interval [-0.2 rad, 0.2 rad]. It is measured with respect to the vertical through a micro strain FAS-G inclinometer. The inertia wheel angular position is measured by an encoder linked to the actuator of the system (Maxon EC-powermax 30 DC motor), allowing to compute

its velocity in real time. The control approach is implemented using C++ language and the whole system runs under the Ardence RTX real-time OS.

Two experimental scenarios are carried out and discussed. In the first one, the proposed control scheme is implemented in nominal case, without considering any external disturbances. In the second one, the system is subject to external disturbances, to show the robustness of the proposed approach. The same parameters are kept same for both scenarios. The parameters used in experiment are presented in table 2.

Table 2. Summary on control design parameters

Parameter	Value	Parameter	Value
α_1	7.3	$\hat{\theta}_1(0)$	0.16
α_2	3.2	L	10
β	14.05	λ_2	50
K_s	19.09	λ_1	80
m_0	0.213	λ_0	110
g	9.8	I	0.0130

4.1. Scenario 1: Nominal case

Figure 4 presents the response of the position and velocity of the pendulum $\theta_1, \dot{\theta}_1$, and the angular velocity of the inertia wheel θ_2. The RISE controller ensures a good stabilization of the pendulum around its unstable equilibrium point. The evolution of control input is presented in figure 5-(a).

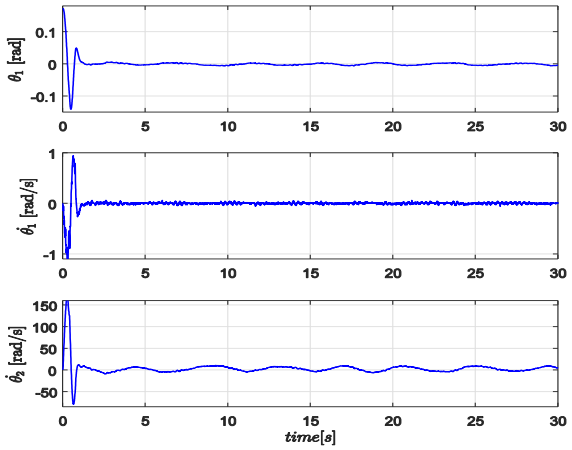

Figure 4. Obtained experimental results for scenario1: Nominal case. Top: Pendulum angular position, Middle: pendulum angular velocity, Bottom: velocity of the inertia wheel

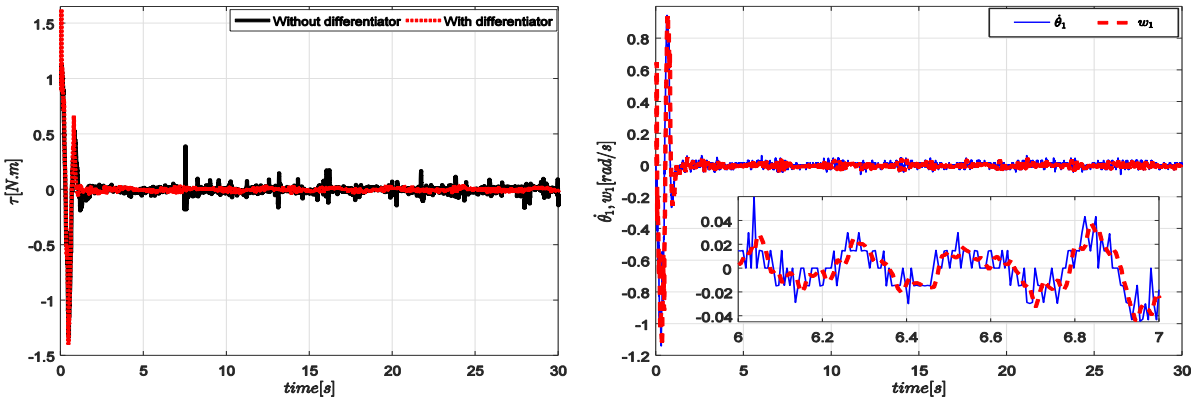

(a) (b)

Figure 5. (a) Evolution of the control input (torque) versus time for scenario1: Nominal case. Solid line: Without HOSM differentiator Dash line: With HOSM differentiator. **(b)** The evolution of the estimated velocity (Dash line) and real measurement of the velocity (Solid line) versus time.

An improvement is observed when the controller is coupled with the HOSM differentiator. Indeed, the control input is depending on the velocity of the pendulum. The latter, is calculated by numerical derivation of the measured angular position of the pendulum, which is in general case contain a noise measurement.
Thus, the noise presented in the control input makes a whirring sound of the actuator and affects the performance of the system. So, the use of the HOSM differentiator, to estimate the position and velocity of the pendulum improves the experimental results.
Known for their robustness in presence of noise, HOSM observer is used in order to provide the derivatives required to implement the RISE controller. In figure 5-(b), the real time measurement velocity (solid line) and estimated angular velocity (dash line) are presented. The plots are zoomed within the interval [6,7] seconds for clarity. The estimated signal is smoother than the computation of the velocity with numerical derivation.

4.2. Scenario 2: Rejection of punctual perturbations

To show the robustness of the proposed controller, the second scenario consists of a disturbing force applied to the body of the pendulum in different time of the experiment. The disturbance is generated by pushing the pendulum at approximately t = 6s, t = 14s and t = 21s. Figure 6 presents the evolution of the system states.

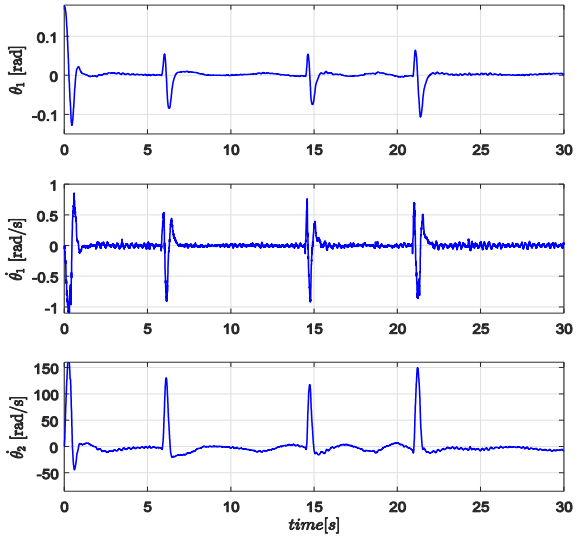

Figure 6. Obtained experimental results for scenario2: Rejection of punctual perturbations. Top: Pendulum angular position, Middle: pendulum angular velocity, Bottom: velocity of the inertia wheel versus time.

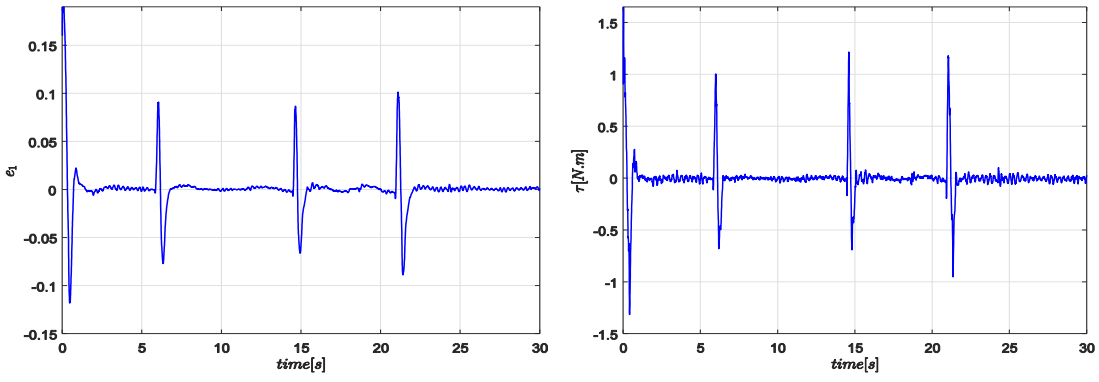

(a) (b)

Figure 7. Scenario 2: Rejection of punctual perturbations **(a)** Evolution of tracking error e_1 versus time. **(b)** Evolution of the control input (torque) versus time.

The effect of the punctual disturbances can be observed as peaks on the curves that appear at instants of application of the disturbing torques. The RISE controller is able to compensate the perturbations and maintain the system around the desired unstable equilibrium point. The evolution of the tracking error e_1 versus time is presented in figure 7-(a). It

converges to zero after each perturbation. The controller is robust with respect to disturbance and performs an accurate stabilization of the inertia wheel inverted pendulum. Figure 7-(b) shows the evolution of the control input versus time.

5. Conclusion and Future Work

In the present paper, we propose a robust control approach for class I of underactuated systems. This class is characterized by one control input and two degrees of freedom. The control approach consists on transformation of the system in strict feedback form. Then novel desired trajectories were designed for the design of the RISE controller. To overcome, the problem of noisy measurement in experimental results, a HOSM differentiator was used to estimate the first derivative of the angular position. This method gives better results than the numerical computation of the first derivative. Real time experiment was conducted in the inertia wheel inverted pendulum to show the efficiency of the controller with respect to unmatched disturbances.

The future work is ongoing to apply the RISE controller, on other class of underactuated mechanical systems. We can also use other extinction of the RISE control approach in order to improve the robustness of the IWIP.

References

[1] A. Choukchou-Braham, B. Cherki, M. Djemai, K. Busawon, Analysis and Control of Underactuated Mechanical Systems, Springer International Publishing Switzerland, 2014.
[2] D. Seto and J. Baillieul, Control problems in super-articulated mechanical systems, IEEE Transactions on Automatic Control, Vol 39, No. 12, pp. 2-2453, 1994.
[3] R. Olfati-Saber, Nonlinear Control of Underactuated Mechanical Systems with application to robotics and aerospace vehicles. PhD thesis, Massachusetts Institute of Technology, 2001.
[4] M. W. Spong, L. Praly, Control of Underactuated Mechanical Systems Using Switching and Saturation, In: Stephen Morse A. (eds) Control Using Logic-Based Switching. Lecture Notes in Control and Information Sciences, vol 222. Springer, Berlin, Heidelberg, 1997.
[5] R. Ortega, M. W. Spong, F. G´omez-Estern and G. Blankenstein, Stabilization of a class of underactuated mechanical systems via interconnection and damping assignment, IEEE Transactions, On Automatic Control, Vol. 47, No. 8, pp. 1213-1233, 2002.
[6] A. Donaire, J .G. Romero, R. Ortega, B. Siciliano and M. Crespo, Robust IDA-PBC for underactuated mechanical systems subject to matched disturbances, International Journal of Robust and Nonlinear Control, vol 27, No. 6, pp. 1000-1016, 2017.
[7] J. Moreno-Valenzuela, C. Aguilar-Avelar, S. Puga-Guzmán and V. Santibánez, Two adaptive control strategies for trajectory tracking of the inertia wheel pendulum: neural networks vis a vis model regressor, Intelligent Automation and Soft Computing, pp.63-73, 2016.
[8] S. Andary, A. Chemori, and S. Krut, Control of the Underactuated Inertia Wheel Inverted Pendulum for Stable Limit Cycle Generation, RSJ Advanced Robotics 23, pp. 1999-2014, 2009.
[9] N. Sun, Y. Fang, and H. Chen, A novel sliding mode control method for an inertia wheel pendulum system, Proceedings of the 2015 International Workshop on Recent Advances in Sliding Modes, Turkey, 2015.
[10] B. Lu, Y.Fang and N. Sun, Global stabilization of inertia wheel systems with a novel sliding mode-based strategy, 14th International Workshop on Variable Structure Systems, Nanjing, China, 2016.
[11] N. Khalid, A. Y. Memon, Output feedback control of a Class of under-actuated nonlinear systems using extended high gain observer, Arab J Sci Eng (2016), vol. 41, No. 9, pp. 3531-3542, 2016.
[12] B. Xian, D.M. Dawson, M.S. de Queiroz, and J. Chen, A continuous asymptotic tracking control strategy for uncertain nonlinear systems. IEEE Transactions on Automatic Control, 49(7):1206–1211, July 2004.
[13] N. Fischer, N. Hughes, D. Walters, P. Schwartz, E. M. and W. E Dixon. Nonlinear RISE-Based Control of an Autonomous Underwater Vehicle, IEEE Transactions on Robotics, 30, 845-852, 2014.
[14] L. Jian, T. Wen and S. Fuchun. Adaptive RISE control of a multi-link flexible manipulator based on integral manifold approach, International Conference on Multisensor Fusion and Information Integration for Intelligent Systems (MFI), Beijing, China , 2014.
[15] M. Bennehar, A. Chemori, M. Bouri, L.F. Jenni and F. Pierrot. A new RISE-based adaptive control of PKMs: design, stability analysis and experiments, International Journal of Control, 91:3, 593-607, 2018, DOI: 10.1080/00207179.2017.1286536.
[16] M. Taktak-Meziou, A. Chemori, J. Ghommam and N. Derbel, A prediction-based optimal gain selection in RISE feedback control for hard disk drive, 2014 IEEE Conference on Control Applications (CCA), Juan Les Antibes, 2014.